

An SOC Estimation System for Lithium ion Batteries Considering Thermal Characteristics

Ryu Ishizaki, Lei Lin, Naoki Kawarabayashi, Masahiro Fukui

Graduate School of Science and Engineering, Ritsumeikan University,
Kusatsu, SHIGA, 525-8577 Japan
Email: mfukui@se.ritsumei.ac.jp

Abstract - This paper discusses an SOC estimation system for lithium ion batteries based on the Extended Karman Filter. The accuracy of the estimation is strongly dependent on accuracy of the battery model. We have newly formulated the equivalent circuit model that considers temperature and SOC dependencies. As the result, the error rate of the estimation has been improved significantly. The evaluation shows that the new SOC estimation system can be used for wide range of temperature.

I. Introduction

In recent decades, invention of the Li-ion battery has opened a new vista of high energy density storages for smart communities. At the same time, an efficient management system for the Li-ion battery is strongly demanded for longer life time and safety. In order to manage the battery effectively, the characteristics and state of the battery must be grasped definitely. Especially, the charge state of the battery, SOC (State of Charge) is an important parameter. The Extended Kalman Filter, which is one of the recursive filters, was reported as an effective technique [1, 2] as a high precision SOC estimation technique of a lithium ion storage battery. Compared with the conventional techniques, such as OCV[3], internal resistance method[4], current accumulation method[5], etc., The Extended Kalman Filter attains higher accuracy [6] However the accuracy of the algorithm strongly depends on the accuracy of the battery model. The battery model includes the open circuit voltage, OCV, and the internal impedance. Furthermore those model parameters vary depending on the battery states, SOC, temperature and degradation. Thus, it is important to consider the temperature and SOC dependencies of internal impedance for accurate SOC estimation. We consider the dynamic change of temperature and SOC in this paper. Consideration of degradation will be solved in the future research. We calibrate the internal parameter of the Li-ion battery using the impedance measuring equipment and decide each parameter in the equivalent model of the battery. Then, we have newly formulated the equivalent circuit model that considers temperature and SOC dependencies. Expression for the temperature dependence is made with Arrhenius formula, and the way to find the accurate parameters of the Arrhenius formula is explained. We apply the Extended Karman filter for the accurate model. Experimental results show the new method is very accurate for the wide range of temperature.

II. Storage Battery Characteristic

Internal reaction of Li-ion battery is expressed by the resistance and capacitance. Such a reaction is able to be expressed as an equivalent circuit model of Li-ion battery as shown in Fig.1[7]. These circuit parameters changes by the temperature and SOC of the battery. Thus, formulating the dependency of them leads to an accurate SOC estimation.

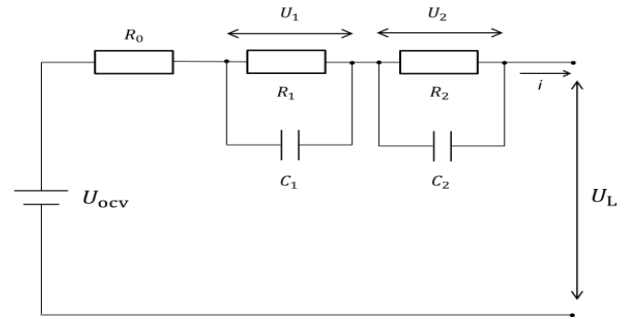


Fig.1 The equivalent circuit model of a battery

$U_{OCV}(V)$ supposes electromotive force. $U_L(V)$ is the voltage between the terminal of the equivalent circuit model. $u_1(V)$ and $u_2(V)$ is a potential difference of the two RC circuit. $I(A)$ is current which flows into a battery. The current which flows into two RC circuits can be expressed as follows.

$$C_1 \frac{du_1}{dt} + \frac{u_1}{R_1} = i \quad (1)$$

$$C_2 \frac{du_2}{dt} + \frac{u_2}{R_2} = i \quad (2)$$

The voltage of the RC circuit when charging and discharging includes the influence by concentration polarization, and is as follows.

$$u_1 = iR_1 \left(1 - e^{-\frac{t}{\tau_1}}\right) \quad (3)$$

$$u_2 = iR_2 \left(1 - e^{-\frac{t}{\tau_2}}\right) \quad (4)$$

$U_L(V)$ can be denoted by the following formulas [8].

$$U_L = OCV(SOC) + iR_0 + u_1 + u_2 \quad (5)$$

III. Internal parameter measurement experiment

It is necessary to grasp the SOC dependence and temperature characteristics of an internal parameter in the equivalent circuit model of the lithium ion storage battery described in Chapter II. Therefore, we measure the AC impedance by changing the environmental temperature from 0 to 45 degree. SOC1.0 represents fully charged state, SOC0 represents the empty state.

A. Experiment environment

The performance of the lithium ion storage battery used for the experiment is shown in TABLE.1.

TABLE.1
The performance table of the battery used

The nominal voltage		3.6V
The nominal capacity		2250mAh
The upper limit voltage		4.2V
The lower limit voltage		3.0V
Size	Diameter	Maximum 18.6mm
	Height	Maximum 65.2mm
Battery type(state)		18650type(new)

At first we perform impedance measurement of a battery of SOC1.0 in the range of frequency 3kHz - 0.08Hz in each environmental temperature. The next to reduce SOC 0.1, and left for 3 hours in order to wait for the voltage recovery. Finally, we perform impedance measurement. we repeat this process until the voltage becomes 3.0V and show an experiment condition in TABLE.2.

TABLE.2
Impedance experimental condition

Environmental temperature	0 - 45°C
The setting voltage	3.0~4.2V
Discharge current	1.125A(0.5C)
AC current	8% of discharge current
Setting frequency	3000~0.08Hz

B. Internal parameter measurement result

An example of the measurement result in each temperature is shown in Fig.2 .

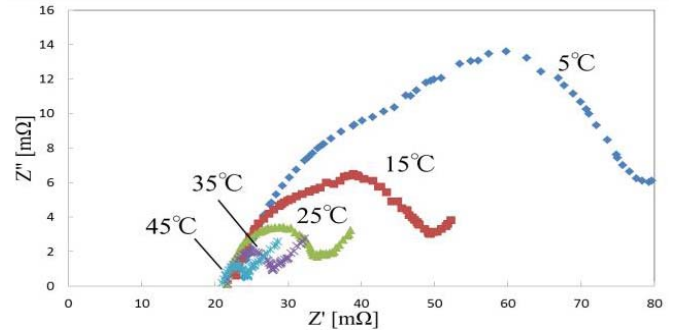


Fig.2 Nyquist plots for dependent temperatures

Fig.2 represents the results of measuring the resistance and capacitance of the battery at each temperature. This is called the Nyquist plot. The horizontal axis represents the resistance, and the vertical axis represents the reactance. We explain this figure about correspondence with equivalent circuit model. R_0 in the equivalent circuit be able to be read from the point in which the reactance is zero. R_1 and R_2 in the equivalent circuit be able to be read from the diameter of the semicircle depicted. Also, capacitive be able to be determined by $C = \frac{1}{2\pi Rf}$. However, only one semicircle is plotted in Fig.2. Therefore, R_2C_2 is difficult to read and is not able to obtain a definite measured value. But the way is described in D of Chapter III because there is a corrective action. The summarize values of each parameter in the graph in the above procedure is shown in Figure.3-5.

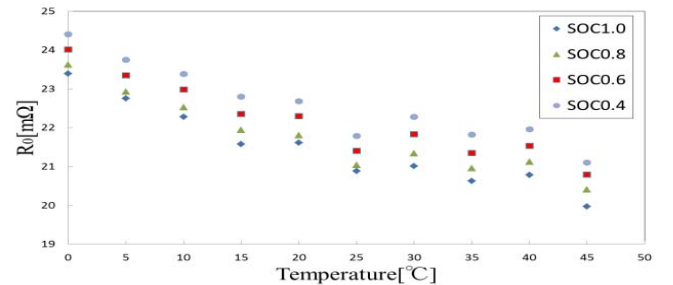


Fig.3 Temperature dependency of impedance parameter R_0

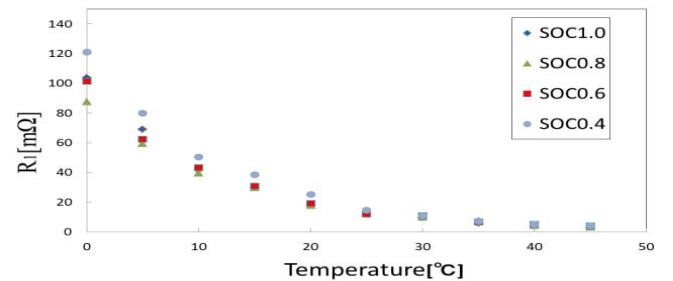


Fig.4 Temperature dependency of impedance parameter R_1

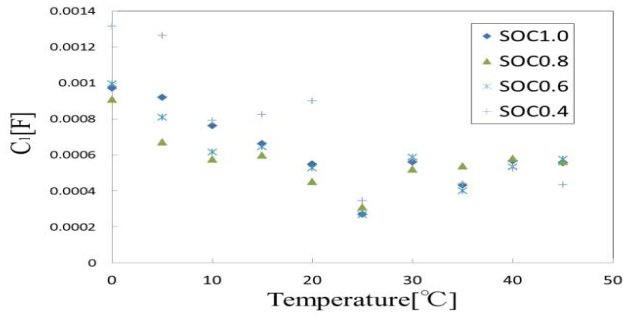


Fig.5 Temperature dependency of impedance parameter C_1

Since the 18650 type of battery manufacturing variability is extremely small manufacturing variations can be ignored.

C. Internal parameter formulization(R_0, R_1, C_1)

Since the reaction inside a storage battery is a chemical reaction, change of the internal parameter assumed that Arrhenius Law was followed. It formulized using Arrhenius' equation ($A \times e^{\frac{B}{RT}}$ (A: A contains a SOC variable R: The constant value for a gas, T: Absolute temperature)). We formulized it by the multiplication of SOC function and the temperature function to formulate in clear form. Therefore A is including the SOC variable. The A procedure of formulation is described taking R_0 for instance. In each SOC, A and B are approximated by a least-squares method using Arrhenius' equation based on the result of impedance measurement. The approximated result is shown in Fig.6-7. Vertical axis expresses the value of the coefficient and the horizontal axis expresses SOC.

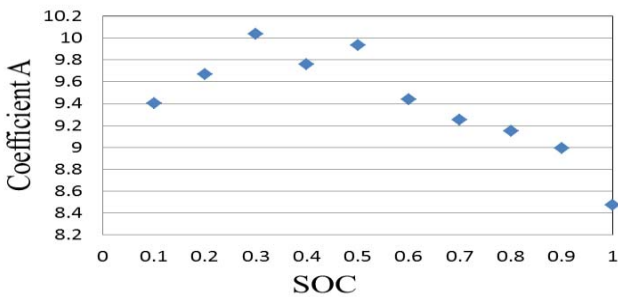


Fig.6 The coefficient A for every SOC

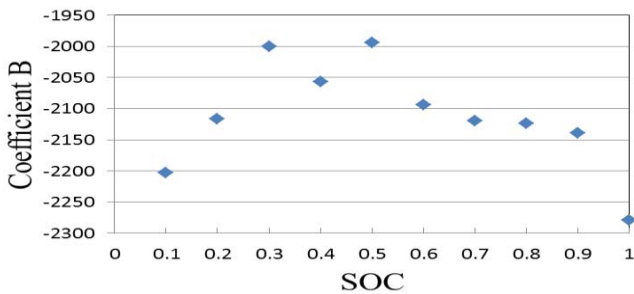


Fig.7 The coefficient B for every SOC

As described above, it is necessary to include the SOC dependency among the A. Therefore, the B must be a constant. Thus, we take the average of the values of B. Its value is adopted as the true value of the B. Finally, the A is approximated by the least square method using the equation again above Arrhenius while fixing the B true value. The result is shown in Fig. 8. Vertical axis expresses the value of the A and the horizontal axis expresses SOC.

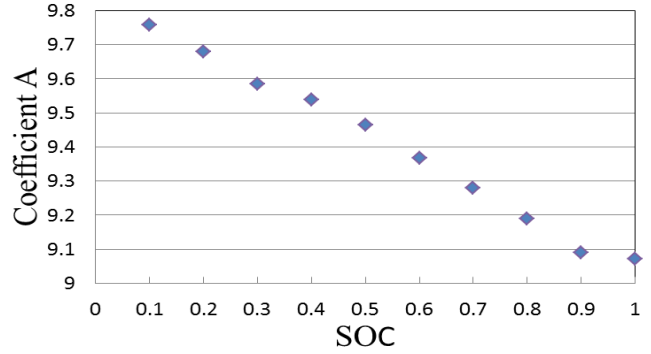


Fig.8 The coefficient A for every SOC after fixing B

The value of Fig.8 is approximated by SOC variable. In such a procedure, we have created a formula that includes a temperature variable and SOC variable. It formulized also about $R_1 C_1$ in the same procedure. R_1 and C_1 are performed formulized also using the same procedure. The fitting result of the final coefficients A and B are shown in TABLE.3.

TABLE.3
Fitting result(R_0 and $R_1 C_1$)

R_0	A	$-0.798282 \times \text{SOC} + 9.841551$
	B	-2112.45
R_1	A	$7.38E-09 \times \text{SOC}^2 - 1.17E-08 \times \text{SOC} + 7.66E-09$
	B	-54819.34
C_1	A	$-1.19E-05 \times \text{SOC}^3 + 3.06E-05 \times \text{SOC}^2 - 2.53E-05 \times \text{SOC} + 8.58E-06$
	B	-13973.80

D. Internal parameter formulization($R_2 C_2$)

As described above, $R_2 C_2$ is difficult to measure by using an AC impedance measuring device. $R_2 C_2$ also assumed to follow the Arrhenius law and formulized using the Arrhenius equation. We explain a formulation procedure of $R_2 C_2$. First of all, we find the coefficient A and B, such as error is reduced by simulation at each temperature. Then, the value of the ideal $R_2 C_2$ calculated by using the A and B is summarized in Table. Finally, it is assumed that the results obtained by measuring the this table, we will conduct the formulation as well as the procedure was carried out in R_0 and $R_1 C_1$. The A and B in the equation of Arrhenius used for $R_2 C_2$ is shown in TABLE.4.

TABLE.4 Fitting result(R_2C_2)

R_2	A	$0.54 \times \text{SOC}^2 + 0.86 \times \text{SOC} + 0.56$
	B	1518.42
C_2	A	$-7.53\text{E-}12 \times \text{SOC}^3 + 1.93\text{E-}11 \times \text{SOC}^2 - 1.60\text{E-}11 \times \text{SOC} + 5.42\text{E-}12$
	B	5071.15

These formulas formed into the formula type are used as an internal parameter in the algorithm of the extended Kalman filter used for the residual quantity prediction described in Chapter IV.

IV. Extended Kalman filter

A Kalman filter is the technique of reducing the target noise component by presuming the following state from a state with the system for observation[9]. To use the Kalman filter is needed two expressions. One is a state equation such as equation (6) that connects the state of the current and the state before one step of the system. Another is an observation equation such as equation (7) that connects the observation value in a certain step and the state of system.

$$x_{k+1} = f(x_k) + \mathbf{b}_u u_k + \mathbf{b} \omega_k \quad (6)$$

$$y_k = h(x_k) + v_k \quad (7)$$

Equation (6) is state equation and equation (7) is observation equation. $f(x_k)$ is the functional relationship of the state vector x_k and the next sample time x_{k+1} . $h(x_k)$ is the functional relationship of the state vector x_k and observation vector y_k . u_k is control vector, ω_k is the process noise, v_k is the observation noise. \mathbf{b}_u and \mathbf{b} are the process vector. When equation (6) and (7) to adapt to the equivalent circuit model of the battery, they become equation (8) and (9).

$$x(k+1) = \begin{bmatrix} \text{SOC}(k+1) \\ u_1(k+1) \\ u_2(k+1) \end{bmatrix} = \begin{bmatrix} 1 & 0 & 0 \\ 0 & \left(1 - \frac{\Delta t}{R_1 C_1}\right) & 0 \\ 0 & 0 & \left(1 - \frac{\Delta t}{R_2 C_2}\right) \end{bmatrix} \times \begin{bmatrix} \text{SOC}(k) \\ U_1(k) \\ U_2(k) \end{bmatrix} \quad (8)$$

$$+ \begin{bmatrix} \frac{\Delta t}{C} \\ \frac{\Delta t}{C_1} \\ \frac{\Delta t}{C_2} \end{bmatrix} \times i(k) + \mathbf{b} \omega(k)$$

$$y(k) = U_L(k) = \text{OCV}(\text{SOC}) + i(k)R_0(\text{SOC}, T) + U_1(k) + U_2(k) + v_k \quad (9)$$

In this model, equation (8) is linear equation, but the OCV(SOC) function is nonlinear equation in equation (9). Therefore, the battery's Discrete-time stochastic model is a nonlinear model. The Kalman filter cannot process a nonlinear model, thence, linearized process method is necessary. Using partial differential, linearize this battery model as equations (10) and (11). Because the state equation is linear equation, the partial differential of the state equation is a constant matrix as Equation (8). Internal parameters of R_0 and $R_1 C_1$ and $R_2 C_2$ equation (8) and (9) use what was formulated as described in Chapter III.

$$\widehat{A}_k = \left. \frac{\partial f(x_k, u_k)}{\partial x_k} \right|_{x_k = \widehat{x}_k} = \begin{bmatrix} 1 & 0 & 0 \\ 0 & \left(1 - \frac{\Delta t}{R_1 C_1}\right) & 0 \\ 0 & 0 & \left(1 - \frac{\Delta t}{R_2 C_2}\right) \end{bmatrix} \quad (10)$$

$$\widehat{C}_k = \left. \frac{\partial h(x_k)}{\partial x_k} \right|_{x_k = \widehat{x}_k} = \left[\frac{d\text{OCV}}{d\text{SOC}} + \frac{dR_0}{d\text{SOC}} \times i_k \Big|_{\text{SOC}=\widehat{\text{SOC}}}, 1, 1 \right] \quad (11)$$

The number of beginning to measure the observed value is the initial state, it is intended that the noise is applied to its true value. We estimate the next state by calculating state model and observation model. The error between the estimated value and the observed value is calculated, and adds the value to the next step. At the same time covariance of error is also updated[10]. We perform a residual quantity prediction by performing this processing until the observation end.

V. SOC presumption simulation

A. Simulation conditions

We performed SOC estimated simulation using MATLAB. Temperature is changed from 15°C to 45°C, and random current as shown in Fig. 9 is sent until it reaches minimum voltage from a full charge state. The voltage value in that case, a current value, and SOC are recorded, and those data is used as simulation input data on MATLAB. The SOC predicted value which the simulation at that time outputted is compared with the value of SOC which a charge-and-discharge machine measures. Experimental simulation conditions are shown in TABLE.5

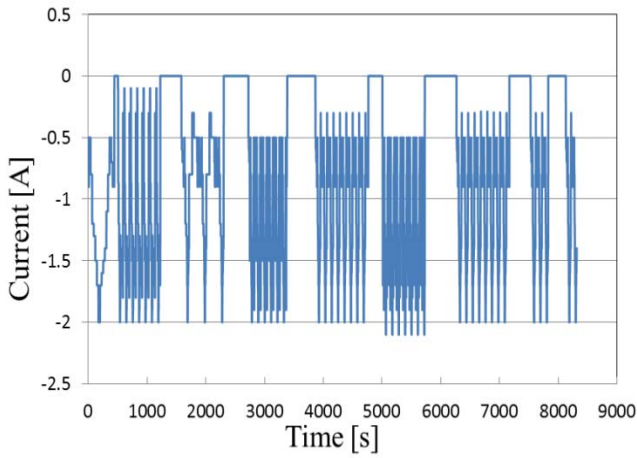


Fig.9 Discharge current

TABLE.5
Simulation conditions

Environmental temperature	15, 25, 35, 45°C
DOD	100%
The lower limit voltage	3.00V
Discharge current	Random pulse
Battery type(state)	18650type(new)

B. Simulation result

The simulation result in each temperature is shown in Fig. 10-13. It is comparing as what nothing is taking into consideration (No consideration), the thing in consideration of three parameters of R_0 and R_1C_1 (Partial consideration) and the thing in consideration of all the parameters included to R_2C_2 (All consideration). The vertical axis represents time. The horizontal axis represents the error rate of the estimated value and the true value.

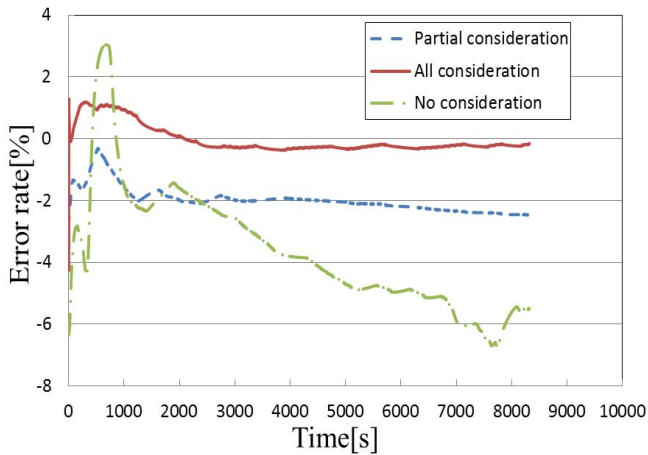


Fig.10 15°C Error rate comparison

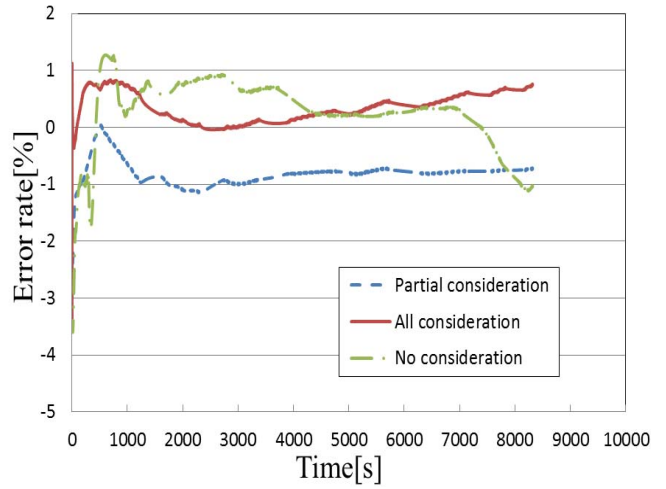


Fig.11 25°C Error rate comparison

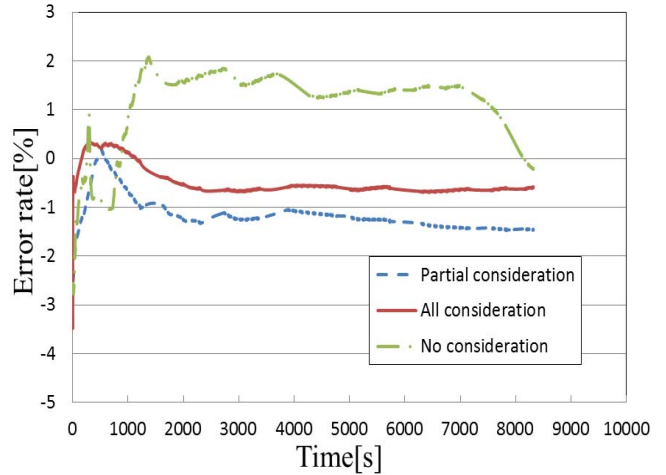


Fig.12 35°C Error rate comparison

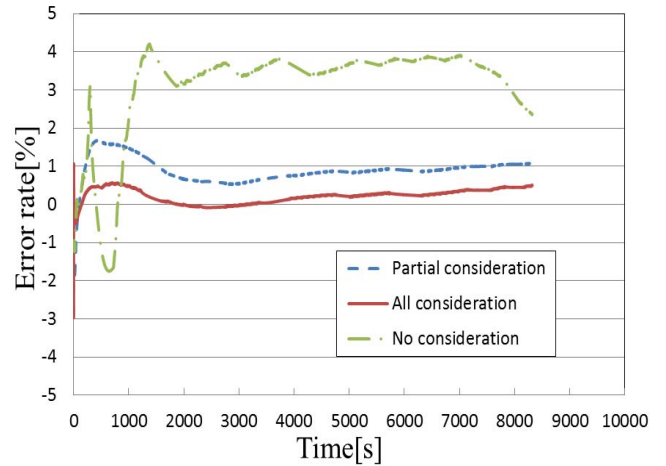


Fig.13 45°C Error rate comparison

The average error rate for each temperature are shown in TABLE 6 and Fig.14.

TABLE.6
Average error rate

	No consideration	Partial consideration	All consideration
15°C	3.84%	1.98%	0.38%
25°C	0.57%	0.81%	0.48%
35°C	1.21%	1.16%	0.54%
45°C	3.00%	0.90%	0.31%

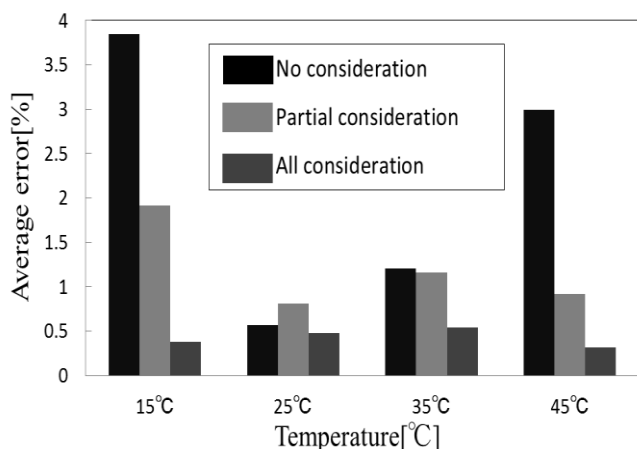


Fig.14 Improvement of error rates

When Fig.14 is seen, Partial consideration is accurate compared with No Consideration. However, No Consideration has better precision than Partial consideration at 25°C. The reason is that the value of the internal parameter is used for No consideration is directly due to the use of a value measured at 25°C. The result of All consideration shows a residual quantity estimate result having very high precision. But not shown in the results, the average error rate at 5°C was 5%. It's because internal reaction of battery is greatly different in low temperature. It is necessary for us to establish a different model for low temperature to be improved. Moreover, it is expected accuracy to be able to grasp R_2C_2 .

VI. Conclusions

The internal impedance of the storage battery was measured. The temperature dependency was well formulated by Arrhenius' equation. The Extended Kalman filter was applied to the SOC estimation for the above model. Compared with the conventional techniques [2], accuracy improvement is significant, and the error rate brought less than 1.0% of highly precise result for temperature range of 15°C – 45°C. Unfortunately, for temperatures less than 5°C, our approach did not succeeded to get good results. As discussed in major battery conferences, we need a different model for low temperature. Thus, we continue to research those low temperature models, too. Since this technique can also be applied to the storage battery temperature change of charge

and discharge, it can obtain a more precise SOC estimation result by combining with the storage battery internal temperature estimation method.

ACKNOWLEDGEMENT

This research is partially supported by NEDO Innovation Commercialization Venture Support Program.

References

- [1] H. Dai, X. Wei, and Z. Sun, "Online SOC estimation of high-power lithium-ion batteries used on HEVs," *IEEE ICVES*, pp. 342-347, 2006.
- [2] L. Lin, N. Kawarabayashi, M. Fukui, S. Tsukiyama, and I. Shirakawa, "A practical and accurate SOC estimation system for lithium ion batteries by EKF," *IEEE VPPC*, 2014.
- [3] G. Wu, R. Lu, C. Zhu, and C.C.Chan, "State of charge estimation for NiMH battery based on electromotive force method," *in Proc. VPPC*, pp.1-5, 2008.
- [4] F. Pei, K. Zhao, Y. Luo, and X. Huang, "Battery variable current-discharge resistance characteristics and state of charge estimation of electric vehicle," *in Proc. WCICA*, pp.8314-8318, 2006.
- [5] F. Baronti, G. Fantechi, L. Fanucci, E. Leonardi, R. Roncella, R. Saletti, and S. Saponara, "State-of-charge estimation enhancing of lithium batteries through a temperature-dependent cell model," *in Proc. Applied Electronics(AE)*, pp.1-5, 2011.
- [6] G. L. Plett, "Extended Kalman filtering for battery management systems of LiPB-based HEV battery packs Part 2. Modeling and identification," *Journal of Power Sources*, vol.134, pp.262–276, 2004.
- [7] M.Chen, and G.A.Rincon-Mora, "Accurate electrical battery model capable of predicting runtime and I-V performance," *IEEE Trans. On Energy Conversion*, vol.21, no.2, pp.504-511, 2011.
- [8] L.Chnglin, L.Huiju and W.Lifang, "A Dynamic Equivalent Circuit Model of LiFePo4 Cathode Material for Lithium Ion Batteries on Hybrid Electric Vehicles," *Vehicle Power and Propulsion Conference*, pp.1662-1665, 2009.
- [9] M. S. Grewal and A. P. Andrews, "Kalman Filtering, WILEY," *2008Transl. J. Magn. Japan*, vol.2, pp. 740-741, August 1987
- [10] L. Chnglin, T.Zining, and W. Lifang, "SOC estimation of LiFePo4 battery energy storage system," *APPEEC*, pp.1-4, Mar. 2010